RESEARCH PAPER

Oleic Acid Alleviates Periodontitis and Is Associated with Reduced m6A Methylation and NLRP3-Mediated Pyroptosis: A Potential Role for METTL3 Downregulation

Shuwen Pan[1], Cheah Fook Cho[2], Wong Kon Ken[3*]

[1] Department of Medical Microbiology & Immunology, Faculty of Medicine, Universiti Kebangsaan Malaysia (UKM), Kuala Lumpur, MALAYSIA.

[123*]Faculty of Medicine, Universiti Kebangsaan Malaysia (UKM), 56000 Cheras, Kuala Lumpur, Malaysia

*Corresponding author: Wong Kon Ken

*Corresponding email: wkk@hctm.ukm.edu.my

Abstract: (1) **Background:** Periodontitis is a chronic inflammatory disease characterized by destruction of tooth-supporting tissues. Although N6-methyladenosine (m6A) RNA methylation and NLRP3 inflammasome-mediated pyroptosis have been implicated in inflammatory injury, their interplay in periodontitis remains unclear. Oleic acid (OA) has anti-inflammatory activity, but its effects on periodontal inflammation are not fully understood.. (2) **Methods:** Human periodontal ligament cells (hPDLCs) were stimulated with Porphyromonas gingivalis-derived lipopolysaccharide (Pg-LPS) with or without OA. Cell viability, lactate dehydrogenase release, pyroptosis, cytokine secretion, m6A-related regulators, NLRP3 inflammasome-related proteins, and global m6A levels were evaluated. A ligature-induced rat periodontitis model was used to assess alveolar bone loss, histopathology, serum cytokines, and periodontal tissue molecular changes. (3) **Results:** Pg-LPS significantly reduced hPDLC viability to 48.95 ± 5.88% of control and increased lactate dehydrogenase release to 16.10 ± 1.41% and pyroptosis to 24.56 ± 2.15% (all $P < 0.001$), whereas OA restored viability to 84.28 ± 8.37% and reduced pyroptosis to 8.10 ± 1.16% ($P < 0.01$). OA also suppressed inflammatory cytokine release, reduced NLRP3 inflammasome activation, attenuated global m6A elevation, and decreased METTL3 expression. In vivo, OA reduced alveolar bone loss, improved periodontal histopathology, lowered serum inflammatory cytokines, and suppressed periodontal tissue NLRP3 activation and m6A hypermethylation. (4) **Conclusions:** Oleic acid protects against Pg-LPS-induced pyroptosis and periodontal destruction. This protective effect is associated with the restoration of m6A methylation homeostasis and suppression of the NLRP3 inflammasome pathway, suggesting a potential mechanism involving the m6A-NLRP3 axis.

Keywords: Oleic acid; Periodontitis; Pyroptosis; m6A methylation; NLRP3 inflammasome

How to cite this article: Pan S, Cho CF, Ken WK. Oleic Acid Alleviates Periodontitis and Is Associated with Reduced m6A Methylation and NLRP3-Mediated Pyroptosis: A Potential Role for METTL3 Downregulation. Int J Drug Deliv Technol. 2026;16(74s): 62-79. DOI: 10.25258/ijddt.16.74s.10

Introduction

Periodontitis is a highly prevalent chronic inflammatory disease characterized by progressive destruction of tooth-supporting tissues, including the periodontal ligament, alveolar bone, and gingiva[1]. The disease is driven by dysbiotic oral biofilms and dysregulated host immune-inflammatory responses, with *Porphyromonas gingivalis* being recognized as a keystone pathogen[2]. P. gingivalis-derived lipopolysaccharide (Pg-LPS), a major virulence factor, promotes sustained inflammation and alveolar bone resorption by activating immune cells and periodontal ligament cells[3, 4]. Human periodontal ligament cells (hPDLCs), one of the principal resident cell types in the periodontal ligament, play a crucial role in maintaining periodontal tissue homeostasis; their injury and dysfunction are key events in periodontitis pathogenesis[5]. Despite advances in mechanical debridement and antimicrobial therapies, effective management of periodontitis remains challenging, necessitating the development of host-modulating therapeutic strategies[6].

Pyroptosis, a pro-inflammatory form of regulated cell death, has recently emerged as a critical mechanism in periodontitis pathogenesis[7]. This process is primarily mediated by gasdermin D (GSDMD) following cleavage by activated caspase-1 downstream of inflammasome assembly[8]. The NOD-like receptor protein 3 (NLRP3) inflammasome, a multiprotein complex consisting of NLRP3, apoptosis-associated speck-like protein containing a CARD (ASC), and pro-caspase-1, responds to microbial and danger signals by activating caspase-1 and thereby promoting the maturation and secretion of interleukin (IL)-1β and IL-18[9]. Accumulating evidence has shown that Pg-LPS activates the NLRP3 inflammasome and induces pyroptosis in hPDLCs, which may represent a critical mechanism underlying periodontal tissue inflammation and damage[10].

N6-methyladenosine (m6A) is the most abundant internal modification of eukaryotic mRNA and plays important roles in RNA metabolism, including splicing, stability, and translation[11]. The m6A landscape is dynamically regulated by methyltransferases ("writers") including methyltransferase-like 3 (METTL3), methyltransferase-like 14 (METTL14), Wilms tumor 1-associated protein (WTAP), and RNA binding motif protein 15 (RBM15), as well as demethylases ("erasers") such as fat mass and obesity-associated protein (FTO) and AlkB homolog 5 (ALKBH5)[12]. Emerging studies have implicated m6A modification in various inflammatory diseases by regulating immune cell function and cytokine expression[13, 14]. Notably, METTL3-mediated m6A methylation has been shown to promote NLRP3 inflammasome activation in macrophages by enhancing NLRP3 mRNA stability[15]. However, whether m6A methylation contributes to pyroptosis in periodontitis and how it interacts with the NLRP3 inflammasome pathway in periodontal cells remain poorly understood.

Oleic acid (OA), an 18-carbon monounsaturated fatty acid abundant in olive oil and other dietary sources, possesses well-documented anti-inflammatory and cytoprotective properties[16, 17]. OA has been shown to modulate immune responses and protect against inflammatory damage in various disease models, including colitis, osteoarthritis, and cardiovascular diseases[18-20]. In the context of oral health, OA has been reported to inhibit the growth of oral pathogens and reduce inflammatory responses in gingival cells[21]. However, its effects on Pg-LPS-induced hPDLC injury and periodontitis, as well as its potential regulatory role in m6A methylation and NLRP3-mediated pyroptosis, have not been fully elucidated.

In this study, we examined the hypothesis that OA protects against Pg-LPS-induced pyroptosis in hPDLCs and in a rat periodontitis model by modulating m6A methylation and inhibiting NLRP3 inflammasome activation. Our findings suggest an association between m6A modification and pyroptosis in periodontitis and support OA as a potential therapeutic agent targeting this pathway, thereby providing a novel nutritional intervention strategy for periodontitis management.

1. Materials and Methods

2.1. Cell Culture and Treatment

Human periodontal ligament cells (hPDLCs) were purchased from Wuhan Saios Biotechnology Co., Ltd. (Wuhan, China) and maintained in Dulbecco's Modified Eagle Medium (DMEM; WelGENE, Daegu, Republic of Korea) supplemented with 10% fetal bovine serum (FBS; WelGENE) and 1% penicillin-streptomycin (Gibco) at 37°C in a humidified atmosphere containing 5% CO_2. Cells at passages 3–8 were used for all experiments.

For stimulation experiments, hPDLCs were seeded in 6-well plates at 2×10^5 cells/well or in 96-well plates (5×10^3 cells/well) and allowed to reach 70–80% confluence. Cells were then exposed to *Porphyromonas gingivalis*-derived lipopolysaccharide (Pg-LPS; 10 μg/mL; InvivoGen, San Diego, CA, USA) in the presence or absence of oleic acid (OA; 100 μM; Sigma-Aldrich, St. Louis, MO, USA) for 24 h. OA was dissolved in water containing 50 mM NaOH at 70°C and then diluted in culture medium to the indicated concentration. Control cells received an equivalent volume of vehicle prepared in water containing 50 mM NaOH. The concentrations of Pg-LPS and OA were selected on the basis of preliminary dose-optimization experiments and previous reports[16, 22].

2.2. Cell Viability Assay

Cell viability was assessed using the Cell Counting Kit-8 (CCK-8; Dojindo, Kumamoto, Japan) according to the manufacturer's instructions. Briefly, hPDLCs were seeded in 96-well plates at a density of 5×10^3 cells/well. After the indicated treatments, 10 μL of CCK-8 solution was added to each well, followed by incubation for 2 h at 37°C in the dark. Absorbance was measured at 450 nm using a microplate reader (Allsheng, Hangzhou, China). Three independent experiments were performed (n = 3).

2.3. Lactate Dehydrogenase (LDH) Release Assay

Cytotoxicity was evaluated by measuring LDH release using the CytoTox 96® Non-Radioactive Cytotoxicity Assay kit (Promega, Madison, WI, USA) according to the manufacturer's instructions. After the indicated treatments, 50 μL of culture supernatant was transferred to a new 96-well plate and mixed with 50 μL of substrate solution. After 30 min incubation at room temperature in the dark, 50 μL of stop solution was added, and absorbance was measured at 490 nm using a microplate reader (Allsheng, Hangzhou, China). LDH release percentage was calculated relative to maximum LDH release from cells lysed with 1% Triton X-100 using the formula: (experimental absorbance – background absorbance) / (maximum release absorbance – background absorbance) × 100%. Three independent experiments were performed, with each condition tested in triplicate (n = 3).

2.4. Pyroptosis Analysis by Flow Cytometry

Pyroptosis was assessed using the FAM-FLICA® Caspase-1 Assay kit (ImmunoChemistry Technologies, Bloomington, MN, USA) in combination with propidium iodide (PI) staining, following the manufacturer's protocol and a previously described method[23]. Briefly, after the indicated treatments, hPDLCs were collected by trypsinization, washed with PBS, and resuspended in 300 μL of culture medium. Cells were incubated with 10 μL of 30× FAM-FLICA-YVAD-FMK probe for 1 h at 37°C in the dark. After washing twice with apoptosis wash buffer provided in the kit, cells were resuspended in 200 μL of wash buffer and stained with 5 μL of PI for 15 min at room temperature in the dark. Samples were analyzed immediately using a FACSCalibur flow cytometer (BD Biosciences, San Jose, CA, USA), and 10,000 events were acquired for each sample. Data were analyzed with FlowJo software (version 10.8, Tree Star, Ashland, OR, USA). Pyroptotic cells were defined as $FAM\text{-}FLICA^+/PI^+$. Three independent experiments were performed (n = 3).

2.5. Cytokine Measurement by ELISA

Concentrations of IL-1β and IL-18 in cell culture supernatants, and tumor necrosis factor-alpha (TNF-α), IL-1β, IL-6, and IL-18 in rat serum, were quantified using enzyme-linked immunosorbent assay (ELISA) kits (Biolegend, San Diego, CA, USA) according to the manufacturer's instructions. Briefly,

96-well plates pre-coated with capture antibodies were incubated with 100 µL of standards or samples overnight at 4°C. After washing four times with wash buffer, 100 µL of detection antibody was added and incubated for 1 h at room temperature. The plates were then washed, followed by incubation with 100 µL of avidin–horseradish peroxidase (HRP) solution for 30 min. After a final wash step, 100 µL of tetramethylbenzidine (TMB) substrate solution was added and incubated in the dark for 15–20 min. The reaction was terminated by adding 100 µL of stop solution (2 N H_2SO_4). Absorbance was measured at 450 nm and 570 nm as the reference wavelength using a microplate reader (Allsheng, Hangzhou, China). Cytokine concentrations were calculated from standard curves generated with recombinant cytokines. All samples were assayed in duplicate. Cell experiments were independently repeated three times, whereas animal experiments included six rats per group (n = 3 for cell studies; n = 6 for animal studies).

2.6. RNA Extraction and Quantitative Real-Time PCR

Total RNA was extracted from hPDLCs using TRIzol reagent (Invitrogen, Carlsbad, CA, USA) according to the manufacturer's instructions. Briefly, cells were lysed directly in culture plates with 1 mL of TRIzol reagent, followed by chloroform extraction and isopropanol precipitation. RNA pellets were washed with 75% ethanol, air-dried, and dissolved in RNase-free water. RNA concentration and purity were assessed using a NanoDrop 2000 spectrophotometer (Thermo Fisher Scientific, Waltham, MA, USA), and samples with A260/A280 ratios between 1.9 and 2.1 were considered acceptable.

Complementary DNA (cDNA) was synthesized from 1 µg of total RNA with the HiSenScript™ RH(-) RT PreMix kit (iNtRON Biotechnology, Seongnam, Republic of Korea) in a total reaction volume of 20 µL. Reverse transcription was performed at 45°C for 60 min, followed by 95°C for 5 min to inactivate the enzyme.

Quantitative real-time PCR (qRT-PCR) was performed using SYBR Green PCR Master Mix (Applied Biosystems, Foster City, CA, USA) on an ABI 7500 real-time PCR system (Applied Biosystems). Each 20 µL reaction contained 10 µL of SYBR Green Master Mix, 1 µL of cDNA, 0.5 µL each of forward and reverse primers (10 µM), and 8 µL of RNase-free water. The PCR cycling conditions were as follows: initial denaturation at 95°C for 10 min, followed by 40 cycles of 95°C for 15 s and 60°C for 1 min. A dissociation curve analysis was performed at the end of each run to confirm amplification specificity. Primer sequences for the m6A-related genes and the internal reference gene GAPDH are listed in Table 1. Relative gene expression was calculated using the $2^{-\Delta\Delta Ct}$ method with GAPDH as the internal control. Three independent experiments were performed (n = 3).

Table 1. Primer sequences for qRT-PCR.

Gene	Forward Primer (5'→3')	Reverse Primer (5'→3')
METTL3	TTGTCACCACCTTCCGTAGT	CCAGATCAGAGAGGTGGTGTAG
METTL14	AGTGCCGACAGCATTGGTG	AGGAGCAGAGGTATCATAGGAAGC
WTAP	CACCTCCGACCTCTTCTTTG	GACCACTTTCTGCTACTGCTTTC
RBM15	CGGGCTGGTTTATGCCTATCT	GCTGCTGCGTTCTACTACCA
FTO	CTTCAAGGACAACCTGACCTAC	TCTTCCTCCGACTGCTATGA
ALKBH5	CGGCGAAGGAGCTTCGTTAC	CGCCTTGCCGTCATCAATAC
GAPDH	ACAACTTTGGTATCGTGGAAGG	GCCATCACGCCACAGTTTC

2.7. Western Blot Analysis

For cell experiments, hPDLCs were lysed directly in radioimmunoprecipitation (RIPA) buffer (Cell Signaling Technology, Beverly, MA, USA) supplemented with protease inhibitor cocktail (1:100; Sigma-Aldrich) and phosphatase inhibitor cocktail (1:100; Genedepot, Katy, TX, USA). For tissue experiments, frozen periodontal tissue samples (approximately 50 mg) were homogenized on ice

using a tissue grinder in the same lysis buffer, incubated on ice for 30 min, and centrifuged at 14,000× g for 20 min at 4°C. The supernatant was collected, and protein concentrations were determined using the bicinchoninic acid (BCA) protein assay kit (Pierce, Rockford, IL, USA) with bovine serum albumin as standard. Equal amounts of protein (30 μg per lane) were mixed with 5× loading buffer, denatured at 95°C for 5 min, and separated by 10% or 12% sodium dodecyl sulfate-polyacrylamide gel electrophoresis (SDS-PAGE). Proteins were then transferred onto polyvinylidene difluoride (PVDF) membranes (Merck Millipore, Burlington, MA, USA) at 300 mA for 90 min at 4°C. Membranes were blocked with 5% skim milk in Tris-buffered saline containing 0.1% Tween-20 (TBST) for 1 h at room temperature and incubated overnight at 4°C with primary antibodies against NLRP3 (rabbit, 1:1000; Adipogen, San Diego, CA, USA), ASC (mouse, 1:1000; Adipogen), active caspase-1 (p10; rabbit, 1:500; Novus, Littleton, CO, USA), GSDMD-N (rabbit, 1:1000; Abcam, Cambridge, UK), METTL3 (rabbit, 1:1000; Abcam), and GAPDH (mouse, 1:3000; Santa Cruz Biotechnology, Santa Cruz, CA, USA). After washing three times with TBST (10 min each), membranes were incubated with horseradish peroxidase (HRP)-conjugated secondary antibodies (1:2000; Santa Cruz Biotechnology) for 1 h at room temperature. Protein bands were visualized using enhanced chemiluminescence (ECL) reagents (Pierce) and detected with a LAS-4000 Imaging System (Fuji Film, Tokyo, Japan). Band intensities were quantified using ImageJ software (version 1.53t, National Institutes of Health, Bethesda, MD, USA) and normalized to GAPDH. Three independent experiments were performed for cell studies (n = 3), whereas periodontal tissue samples from six rats per group were used for in vivo analysis (n = 6).

2.8. Dot Blot Assay for Global m6A Modification

Global m6A RNA methylation levels were assessed by dot blot assay following a previously described method[24]. Briefly, total RNA was extracted from hPDLCs or periodontal tissues using TRIzol reagent, and RNA concentration was adjusted to 200 ng/μL with RNase-free water. RNA samples (2 μg in 10 μL) were denatured at 95°C for 5 min and immediately chilled on ice for 2 min. Denatured RNA was spotted onto a Hybond-N^+ nylon membrane (GE Healthcare, Chicago, IL, USA) using a 96-well dot blot apparatus. The RNA was crosslinked to the membrane by UV irradiation (254 nm, 5 min) using a UV crosslinker. After air-drying for 10 min, the membrane was blocked with 5% skim milk in TBST for 1 h at room temperature and then incubated overnight at 4°C with rabbit anti-m6A antibody (1:1000; Synaptic Systems, Göttingen, Germany). After washing three times with TBST, the membrane was incubated with HRP-conjugated goat anti-rabbit secondary antibody (1:2000; Santa Cruz Biotechnology) for 1 h at room temperature. Signals were detected using ECL reagents and visualized with a LAS-4000 Imaging System. For loading normalization, equal amounts of RNA were evaluated by methylene blue staining, and dot blot signals were quantified using ImageJ software for normalization. Three independent cell-based dot blot experiments were performed (n = 3), whereas periodontal tissue samples from six rats per group were analyzed for in vivo dot blot assays (n = 6).

2.9. Animal Model of Periodontitis

All animal experiments were approved by the Institutional Animal Care and Use Committee of [University Name] (IACUC No. [XXXXXX]) and were conducted in accordance with the ARRIVE guidelines and the National Institutes of Health Guide for the Care and Use of Laboratory Animals. Six-week-old male Sprague-Dawley rats (weighing 180–220 g) were purchased from [Vendor Name, City, Country]. Rats were housed under specific pathogen-free conditions under a 12 h light/dark cycle at 22 ± 2°C and 50 ± 10% relative humidity, with free access to standard chow and autoclaved water. Animals were allowed to acclimatize for one week before the experiment.

After acclimatization, rats were randomly assigned to three groups (n = 6 per group): a normal control group (Normal), a periodontitis model group (Model), and an oleic acid treatment group (OA). Experimental

periodontitis was induced using a ligature-induced model as previously described[25]. Briefly, rats were anesthetized by intraperitoneal injection of zoletil (30 mg/kg; Virbac, Carros, France) and xylazine (10 mg/kg; Bayer, Leverkusen, Germany). A 3-0 silk suture (Ethicon, Somerville, NJ, USA) soaked in *P. gingivalis* LPS (1 mg/mL) was placed around the maxillary second molars bilaterally and knotted mesially. The ligatures were checked daily and replaced every 3 days under light anesthesia to maintain continuous irritation throughout the 4-week experimental period.

Rats in the OA group received intraperitoneal injections of oleic acid (10 mg/kg/day; Sigma-Aldrich), starting one week before ligature placement (day –7) and continuing throughout the 4-week experimental period until day 28. The OA dose was selected on the basis of previous studies showing anti-inflammatory efficacy without apparent toxicity[26]. Rats in the Normal and Model groups received the corresponding vehicle on the same schedule. Body weight was monitored weekly throughout the experiment.

At the end of the experimental period, rats were anesthetized as described above, and blood samples were collected by cardiac puncture for serum cytokine analysis. The animals were then euthanized by CO_2 inhalation. Maxillae were dissected, cleaned of soft tissue, and fixed in 4% paraformaldehyde for 48 h at 4°C for micro-CT analysis and histological examination. For molecular analyses, periodontal tissues (gingiva and periodontal ligament) were carefully separated from the alveolar bone under a dissecting microscope, snap-frozen in liquid nitrogen, and stored at –80°C until use.

2.10. Micro-Computed Tomography (Micro-CT) Analysis

Maxillary specimens fixed in 4% paraformaldehyde were washed with PBS and scanned using a high-resolution micro-CT system (SkyScan 1272, Bruker, Kontich, Belgium) at 60 kV and 166 μA with a 0.5 mm aluminum filter, a voxel size of 10 μm, a rotation step of 0.5°, and a full 360° rotation. The scanning time was approximately 30 min per sample. Three-dimensional images were reconstructed using NRecon software (version 1.7.4, Bruker) with a beam-hardening correction of 30%, ring artifact reduction of 10, and smoothing of 2.

Alveolar bone loss was assessed by measuring the distance from the cementoenamel junction (CEJ) to the alveolar bone crest (ABC) at the mesial and distal aspects of the maxillary second molars using DataViewer software (version 1.5.6, Bruker). Measurements were obtained from the designated sites for each tooth and averaged. Bone morphometric parameters were further analyzed in a region of interest (ROI) surrounding the maxillary second molar roots using CTAn software (version 1.18, Bruker). The ROI was defined as a cuboidal volume (2 mm × 2 mm × 2 mm) encompassing the interradicular bone. The following parameters were measured: bone volume fraction (BV/TV, %), trabecular thickness (Tb.Th, mm), trabecular separation (Tb.Sp, mm), trabecular number (Tb.N, mm^{-1}), and bone mineral density (BMD, g/cm^3). BMD was calibrated using hydroxyapatite phantoms with known densities (0.25 and 0.75 g/cm^3). All measurements were performed by a single blinded examiner to ensure consistency and impartiality.

2.11. Histological Analysis

Following micro-CT scanning, maxillary specimens were decalcified in 10% ethylenediaminetetraacetic acid (EDTA; pH 7.4) for 4 weeks at 4°C, with the decalcifying solution changed every 3 days. Complete decalcification was confirmed by radiographic examination. Specimens were then dehydrated through a graded ethanol series (70%, 80%, 90%, 95%, and 100% ethanol), cleared in xylene, and embedded in paraffin. Serial sections (5 μm thick) were cut in the mesiodistal plane using a rotary microtome (Leica RM2235, Leica Biosystems, Nussloch, Germany) and mounted on silane-coated slides.

For general morphological assessment, sections were deparaffinized in xylene, rehydrated through graded ethanol, and stained with hematoxylin and eosin (H&E). Briefly, sections were stained with hematoxylin for 5 min, washed in running tap water

for 10 min, counterstained with eosin for 2 min, dehydrated through graded ethanol, cleared in xylene, and mounted with Permount mounting medium (Fisher Scientific, Hampton, NH, USA). Images were captured using a light microscope (Olympus BX53, Olympus, Tokyo, Japan) equipped with a digital camera (DP80, Olympus). Histological evaluation was performed based on inflammatory cell infiltration, periodontal ligament fiber organization, and alveolar bone integrity.

2.12. Immunohistochemistry (IHC)

Immunohistochemical staining was performed to detect METTL3 and NLRP3 expression in periodontal ligament tissues. Paraffin-embedded sections (5-μm-thick) were deparaffinized in xylene and rehydrated through graded ethanol. Antigen retrieval was performed by boiling sections in 10 mM citrate buffer (pH 6.0) for 15 min in a microwave oven (700 W). Sections were allowed to cool to room temperature for 30 min, then washed with PBS. Endogenous peroxidase activity was blocked with 3% H_2O_2 in methanol for 10 min at room temperature. Non-specific binding was blocked with 5% normal goat serum (Vector Laboratories, Burlingame, CA, USA) in PBS for 1 h at room temperature.

Sections were incubated overnight at 4°C with primary antibodies diluted in blocking buffer: rabbit anti-METTL3 (1:200; Abcam) or rabbit anti-NLRP3 (1:200; Adipogen). After washing three times with PBS (5 min each), sections were incubated with biotinylated goat anti-rabbit secondary antibody (1:200; Vector Laboratories) for 1 h at room temperature, followed by avidin-biotin complex (ABC) reagent (Vector Laboratories) for 30 min. Color was developed using 3,3'-diaminobenzidine (DAB) substrate (Vector Laboratories) for 2–5 min, and sections were counterstained with hematoxylin for 30 s. After dehydration and clearing, sections were mounted with Permount mounting medium. Negative controls were processed identically except that the primary antibody was omitted.

Images were captured using a light microscope (Olympus BX53) at 200× and 400× magnification. Staining intensity was quantified using ImageJ software by integrated optical density (IOD) analysis. For each section, five randomly selected fields in the periodontal ligament region were analyzed, and the mean integrated optical density (IOD) was calculated.

2.13. Statistical Analysis

All data are presented as mean ± standard deviation (SD). Statistical analyses were performed using GraphPad Prism software (version 9.5, GraphPad Software, San Diego, CA, USA). Data distribution was assessed for approximate normality using the Shapiro–Wilk test. For multiple group comparisons, one-way analysis of variance (ANOVA) was performed, followed by Tukey's post hoc test for pairwise comparisons. A two-sided P value < 0.05 was considered statistically significant. For cell culture experiments, n = 3 represented three independent biological replicates; for animal studies, n = 6 per group.

2. Results

3.1. Oleic Acid Attenuates Pg-LPS-Induced Cytotoxicity and Pyroptosis in hPDLCs

To evaluate the protective effect of oleic acid (OA) on Pg-LPS-induced injury in hPDLCs, cell viability was first assessed using the CCK-8 assay. Exposure to Pg-LPS (10 μg/mL) for 24 h significantly reduced cell viability to 48.95 ± 5.88% of the control level (Figure 1A, Table 2). Co-treatment with OA (100 μM) markedly restored cell viability to 84.28 ± 8.37%.

Consistent with the decrease in cell viability, LDH release was significantly elevated in the Pg-LPS group (16.10 ± 1.41%) compared with the control group (3.24 ± 0.85%; Figure 1B, Table 2), indicating substantial membrane damage. OA co-treatment reduced LDH release to 5.63 ± 0.57%, suggesting that OA alleviated Pg-LPS-induced cytotoxicity.

To further determine whether pyroptosis was involved, pyroptotic cells were quantified by FAM-FLICA caspase-1/PI flow cytometry. As shown in the representative flow cytometry plots (Figure 1C), Pg-LPS markedly increased the pyroptosis rate to 24.56 ± 2.15%, compared with 4.83 ± 1.49% in the control group (Figure 1D, Table 2). OA co-treatment significantly decreased the pyroptosis rate to 8.10 ±

1.16%. Collectively, these results indicate that OA alleviates Pg-LPS-induced cytotoxicity and pyroptosis in hPDLCs.

Table 2. Effects of OA on Pg-LPS-induced cytotoxicity and pyroptosis in hPDLCs

Parameter	Control	Pg-LPS	Pg-LPS+OA
Cell viability (%)	100.00 ± 8.52	48.95 ± 5.88***	84.28 ± 8.37##
LDH release (%)	3.24 ± 0.85	16.10 ± 1.41***	5.63 ± 0.57##
Pyroptosis rate (%)	4.83 ± 1.49	24.56 ± 2.15***	8.10 ± 1.16##

Data are presented as mean ± SD (n = 3). ***p < 0.001 vs. Control; ##p < 0.01 vs. Pg-LPS.

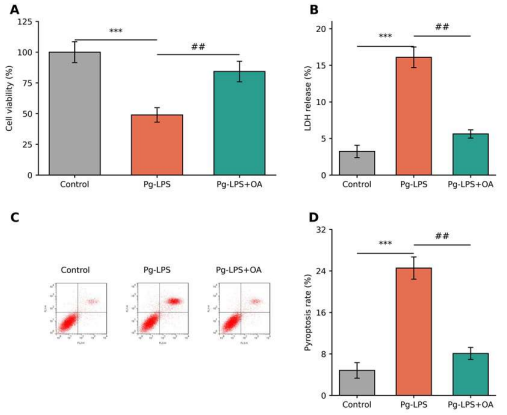

Figure 1. Oleic acid attenuates Pg-LPS-induced cytotoxicity and pyroptosis in hPDLCs. (A) Cell viability measured by CCK-8 assay. (B) LDH release in culture supernatants. (C) Representative flow cytometry plots of FAM-FLICA caspase-1/PI staining in the Control, Pg-LPS, and Pg-LPS+OA groups. (D) Quantification of pyroptosis rate. Data are presented as mean ± SD (n = 3). ***p < 0.001 vs. Control; ##p < 0.01 vs. Pg-LPS.

3.2. OA Suppresses Pg-LPS-Induced Inflammatory Cytokine Secretion in hPDLCs

Because pyroptosis is closely associated with the release of pro-inflammatory cytokines, particularly IL-1β and IL-18, we next quantified their levels in culture supernatants by ELISA. Pg-LPS stimulation markedly increased IL-1β secretion from 65.94 ± 7.62 pg/mL in the control group to 161.66 ± 8.98 pg/mL (P < 0.001; Figure 2A, Table 3). Co-treatment with OA significantly reduced IL-1β levels to 78.27 ± 5.30 pg/mL (P < 0.001 vs. Pg-LPS).

Similarly, IL-18 secretion was significantly elevated in the Pg-LPS group (45.13 ± 3.56 pg/mL) compared with the control group (28.98 ± 2.62 pg/mL, P < 0.01; Figure 2B, Table 3). OA treatment significantly attenuated this increase, reducing IL-18 levels to 30.68 ± 3.46 pg/mL (P < 0.01 vs. Pg-LPS). These findings indicate that OA suppresses Pg-LPS-induced inflammatory cytokine secretion in hPDLCs.

Table 3. Effects of OA on Pg-LPS-induced cytokine secretion in hPDLCs

Cytokine (pg/mL)	Control	Pg-LPS	Pg-LPS+OA
IL-1β	65.94 ± 7.62	161.66 ± 8.98***	78.27 ± 5.30###
IL-18	28.98 ± 2.62	45.13 ± 3.56**	30.68 ± 3.46##

Data are presented as mean ± SD (n = 3). **P < 0.01, ***P < 0.001 vs. Control; ##P < 0.01, ###P < 0.001 vs. Pg-LPS.

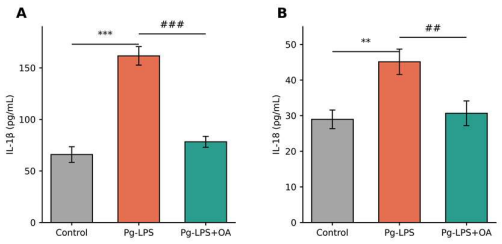

Figure 2. OA suppresses Pg-LPS-induced inflammatory cytokine secretion in hPDLCs. (A) IL-1β levels in culture supernatants measured by ELISA. (B) IL-18 levels in culture supernatants measured by ELISA. Data are presented as mean ± SD (n = 3). **P < 0.01, ***P < 0.001 vs. Control; ##P < 0.01, ###P < 0.001 vs. Pg-LPS.

3.3. OA Inhibits NLRP3 Inflammasome Activation in Pg-LPS-Stimulated hPDLCs

To further investigate the mechanism by which OA attenuated Pg-LPS-induced pyroptosis, we examined the expression of NLRP3 inflammasome-related proteins by Western blot. As shown in Figure 3A, Pg-LPS markedly increased the protein levels of NLRP3, ASC, active caspase-1 (p10), and GSDMD-N in hPDLCs compared with the control

group. Densitometric analysis showed that NLRP3, ASC, active caspase-1 (p10), and GSDMD-N were elevated to 2.85 ± 0.31-fold, 2.42 ± 0.28-fold, 3.12 ± 0.35-fold, and 2.98 ± 0.33-fold of control levels, respectively (Figure 3B).

Co-treatment with OA significantly reduced the expression of these proteins. Specifically, NLRP3, ASC, active caspase-1 (p10), and GSDMD-N were decreased to 1.42 ± 0.18-fold, 1.38 ± 0.15-fold, 1.51 ± 0.19-fold, and 1.45 ± 0.16-fold, respectively, in the Pg-LPS+OA group (Figure 3B). These findings indicate that OA suppresses Pg-LPS-induced activation of the NLRP3 inflammasome and downstream GSDMD cleavage in hPDLCs.

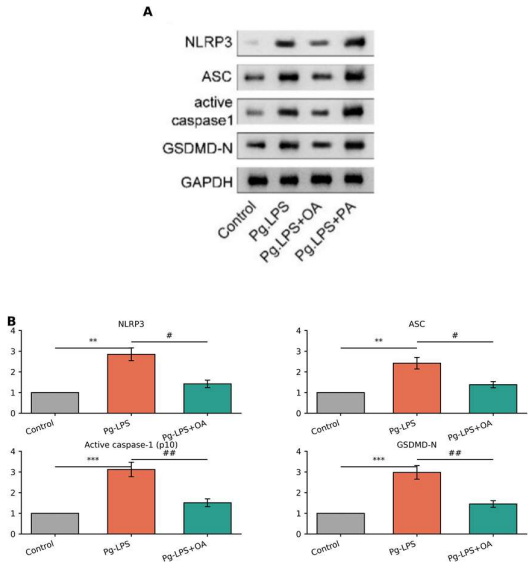

Figure 3. OA inhibits NLRP3 inflammasome activation in Pg-LPS-stimulated hPDLCs. (A) Representative Western blot analysis of NLRP3, ASC, active caspase-1 (p10), GSDMD-N, and GAPDH in hPDLCs. (B) Densitometric quantification of protein bands normalized to GAPDH (n = 3). Data are presented as mean ± SD. **P < 0.01, ***P < 0.001 vs. Control; #P < 0.05, ##P < 0.01 vs. Pg-LPS.

3.4. OA Modulates Global m6A RNA Methylation and m6A-Related Regulators in Pg-LPS-Stimulated hPDLCs

To determine whether the protective effects of OA were associated with changes in m6A RNA methylation, global m6A levels were first assessed by dot blot. Pg-LPS stimulation markedly increased the global m6A signal to 2.56 ± 0.28-fold relative to the control group, whereas OA treatment reduced it to 1.38 ± 0.19-fold (Figure 4A,B). These results indicate that Pg-LPS induced m6A hypermethylation in hPDLCs, which was attenuated by OA.

We next examined the mRNA expression of m6A-related regulators by qRT-PCR. Pg-LPS significantly upregulated METTL3 and METTL14 to 3.08 ± 0.12-fold and 2.10 ± 0.13-fold, respectively, while FTO and ALKBH5 were reduced to 0.52 ± 0.10-fold and 0.83 ± 0.10-fold, respectively (Figure 4C, Table 4). In contrast, WTAP and RBM15 showed no obvious changes among groups. OA treatment significantly reduced METTL3 expression to 1.41 ± 0.14-fold, whereas METTL14 remained elevated at 2.01 ± 0.24-fold. FTO showed only a modest increase to 0.59 ± 0.06-fold, and no recovery of ALKBH5 was observed (0.73 ± 0.04-fold).

Western blot analysis further confirmed that METTL3 protein expression was markedly increased by Pg-LPS to 2.68 ± 0.29-fold and was reduced to 1.35 ± 0.17-fold following OA treatment (Figure 4D,E). Collectively, these findings suggest that OA attenuates Pg-LPS-induced m6A dysregulation in hPDLCs, with suppression of METTL3 representing the most consistent change associated with OA treatment.

Table 4. Effects of OA on m6A regulator mRNA expression in Pg-LPS-stimulated hPDLCs.

Gene	Control	Pg-LPS	Pg-LPS+OA
METTL3	1.00 ± 0.17	3.08 ± 0.12***	1.41 ± 0.14##
METTL14	1.00 ± 0.07	2.10 ± 0.13**	2.01 ± 0.24
WTAP	1.00 ± 0.17	1.05 ± 0.10	1.00 ± 0.04
RBM15	1.00 ± 0.12	0.85 ± 0.06	0.94 ± 0.07
FTO	1.00 ± 0.05	0.52 ± 0.10**	0.59 ± 0.06
ALKBH5	1.00 ± 0.04	0.83 ± 0.10*	0.73 ± 0.04

Data are mean ± SD (n = 3). *P < 0.05, **P < 0.01, ***P < 0.001 vs. Control; ##P < 0.01 vs. Pg-LPS.

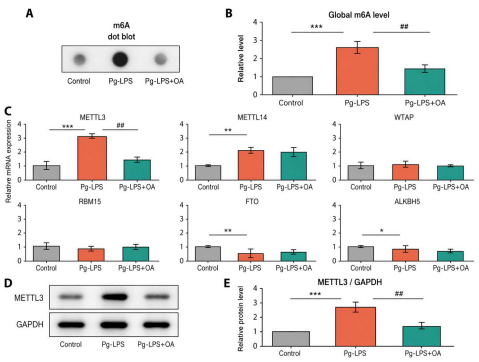

Figure 4. OA modulates global m6A RNA methylation and m6A-related regulators in Pg-LPS-stimulated hPDLCs. (A) Representative dot blot analysis of global m6A levels in hPDLCs. (B) Quantification of relative m6A dot blot signals. (C) qRT-PCR analysis of m6A-related regulators, including METTL3, METTL14, WTAP, RBM15, FTO, and ALKBH5. (D) Representative Western blot analysis of METTL3 protein expression. (E) Densitometric quantification of METTL3 normalized to GAPDH. Data are presented as mean ± SD (n = 3). *P < 0.05, **P < 0.01, ***P < 0.001 vs. Control; ##P < 0.01 vs. Pg-LPS.

3.5. OA Attenuates Alveolar Bone Loss and Improves Periodontal Tissue Integrity in a Rat Periodontitis Model

To evaluate the protective effect of OA in vivo, a ligature-induced rat periodontitis model was established. Micro-CT quantitative analysis showed that the CEJ-ABC distance was significantly increased in the Model group (0.68 ± 0.05 mm) relative to the Normal group (0.39 ± 0.05 mm, P < 0.001), while OA treatment significantly reduced this value to 0.49 ± 0.04 mm (P < 0.05 vs. Model; Figure 5A, Table 5).

Further analysis of bone microarchitecture demonstrated that BV/TV was significantly decreased in the Model group (64.36 ± 3.29%) compared with the Normal group (74.05 ± 4.15%, P < 0.01), and partially restored by OA treatment (71.26 ± 3.31%, P < 0.05 vs. Model; Figure 5B). Trabecular thickness (Tb.Th) was also markedly reduced in the Model group (0.20 ± 0.03 mm) relative to the Normal group (0.35 ± 0.03 mm, P < 0.001), whereas OA treatment significantly increased Tb.Th to 0.30 ± 0.03 mm (P < 0.01 vs. Model; Figure 5C). In contrast, trabecular separation (Tb.Sp) was significantly increased in the Model group (0.16 ± 0.01 mm) compared with the Normal group (0.12 ± 0.01 mm, P < 0.01), and OA treatment reduced Tb.Sp to 0.13 ± 0.02 mm (P < 0.05 vs. Model; Figure 5D). No significant differences in trabecular number (Tb.N) were observed among groups (Figure 5E). In addition, bone mineral density (BMD) was significantly lower in the Model group (0.80 ± 0.06 g/cm³) than in the Normal group (0.97 ± 0.06 g/cm³, P < 0.01), whereas OA treatment increased BMD to 0.90 ± 0.05 g/cm³ (P < 0.05 vs. Model; Figure 5F).

Histological examination by H&E staining further supported these findings. Periodontal tissues in the Normal group showed well-organized periodontal ligament fibers and intact alveolar bone architecture, whereas the Model group exhibited pronounced inflammatory cell infiltration, disorganized periodontal ligament fibers, and obvious alveolar bone destruction. In contrast, OA treatment reduced inflammatory infiltration and preserved periodontal tissue architecture (Figure 5G). Collectively, these findings indicate that OA attenuates alveolar bone loss and improves periodontal tissue integrity in vivo.

Table 5. Effects of OA on alveolar bone parameters in the rat periodontitis model

Parameter	Normal	Model	OA
CEJ-ABC (mm)	0.39 ± 0.05	0.68 ± 0.05***	0.49 ± 0.04#
BV/TV (%)	74.05 ± 4.15	64.36 ± 3.29**	71.26 ± 3.31#
Tb.Th (mm)	0.35 ± 0.03	0.20 ± 0.03***	0.30 ± 0.03##
Tb.Sp (mm)	0.12 ± 0.01	0.16 ± 0.01**	0.13 ± 0.02#
Tb.N (1/mm)	2.34 ± 0.18	2.99 ± 0.27	2.48 ± 0.28
BMD (g/cm³)	0.97 ± 0.06	0.80 ± 0.06**	0.90 ± 0.05#

Data are presented as mean ± SD (n = 6). **P < 0.01, ***P < 0.001 vs. Normal; #P < 0.05, ##P < 0.01 vs. Model.

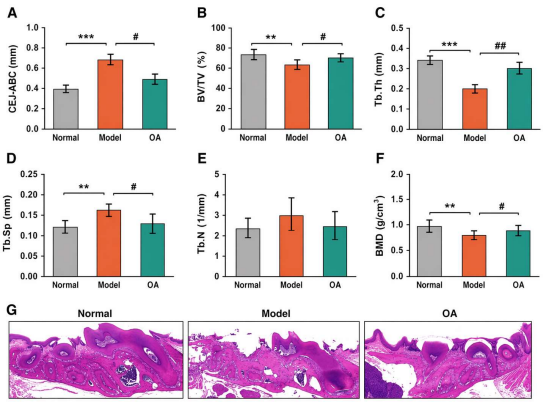

Figure 5. OA attenuates alveolar bone loss and improves periodontal tissue integrity in a rat periodontitis model. (A) Quantification of the distance from the cementoenamel junction to the alveolar bone crest (CEJ-ABC). (B) Bone volume fraction (BV/TV). (C) Trabecular thickness (Tb.Th). (D) Trabecular separation (Tb.Sp). (E) Trabecular number (Tb.N). (F) Bone mineral density (BMD). (G) Representative hematoxylin and eosin (H&E) staining images of periodontal tissues from the Normal, Model, and OA groups. Data in (A–F) are presented as mean ± SD (n = 6). P < 0.01, *P < 0.001 vs. Normal; #P < 0.05, ##P < 0.01 vs. Model.

3.6. OA Suppresses Systemic Inflammation in the Periodontitis Model

To evaluate the anti-inflammatory effect of OA in vivo, serum cytokine levels were measured by ELISA. Compared with the Normal group, the Model group exhibited significantly elevated serum levels of TNF-α, IL-1β, IL-6, and IL-18 (Figure 6A–D, Table 6). Specifically, TNF-α increased from 164.41 ± 16.44 pg/mL in the Normal group to 283.22 ± 28.86 pg/mL in the Model group (P < 0.001), whereas OA treatment reduced it to 226.19 ± 21.44 pg/mL (P < 0.05 vs. Model; Figure 6A).

Similarly, serum IL-1β levels were significantly elevated in the Model group (30.39 ± 3.21 pg/mL) compared with the Normal group (18.86 ± 2.21 pg/mL, P < 0.001), and OA treatment significantly decreased IL-1β to 22.01 ± 1.88 pg/mL (P < 0.01 vs. Model; Figure 6B). Serum IL-6 also increased from 83.31 ± 7.30 pg/mL in the Normal group to 127.89 ± 14.82 pg/mL in the Model group (P < 0.01), and was reduced to 97.52 ± 12.44 pg/mL following OA treatment (P < 0.05 vs. Model; Figure 6C). In addition, IL-18 levels were significantly higher in the Model group (39.78 ± 2.30 pg/mL) than in the Normal group (33.59 ± 1.55 pg/mL, P < 0.01), whereas OA treatment lowered IL-18 to 35.18 ± 2.13 pg/mL (P < 0.05 vs. Model; Figure 6D). These findings indicate that OA suppresses systemic inflammation in the rat periodontitis model.

Table 6. Effects of OA on serum cytokine levels in the rat periodontitis model

Cytokine (pg/mL)	Normal	Model	OA
TNF-α	164.41 ± 16.44	283.22 ± 28.86***	226.19 ± 21.44#
IL-1β	18.86 ± 2.21	30.39 ± 3.21***	22.01 ± 1.88##
IL-6	83.31 ± 7.30	127.89 ± 14.82**	97.52 ± 12.44#
IL-18	33.59 ± 1.55	39.78 ± 2.30**	35.18 ± 2.13#

Data are presented as mean ± SD (n = 6). **P < 0.01, ***P < 0.001 vs. Normal; #P < 0.05, ##P < 0.01 vs. Model.

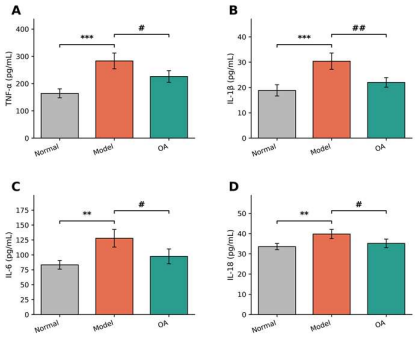

Figure 6. OA suppresses systemic inflammation in the rat periodontitis model. Serum levels of (A) TNF-α, (B) IL-1β, (C) IL-6, and (D) IL-18 were measured by ELISA. Data are presented as mean ± SD (n = 6). **P < 0.01, ***P < 0.001 vs. Normal; #P < 0.05, ##P < 0.01 vs. Model.

3.7. OA Inhibits NLRP3 Inflammasome Activation and m6A Hypermethylation in Periodontal Tissues

To determine whether the protective effects of OA in

vivo involved mechanisms similar to those observed in vitro, we further examined NLRP3 inflammasome-related proteins and m6A modification in periodontal tissues. Western blot analysis showed that NLRP3, ASC, active caspase-1, and GSDMD-N were markedly increased in the Model group compared with the Normal group. Densitometric analysis demonstrated that NLRP3, ASC, active caspase-1, and GSDMD-N were elevated to 2.71 ± 0.29-fold, 2.18 ± 0.24-fold, 2.85 ± 0.31-fold, and 2.62 ± 0.27-fold of the Normal level, respectively (Figure 7A,B). OA treatment significantly reduced the expression of these proteins to 1.45 ± 0.19-fold, 1.35 ± 0.16-fold, 1.52 ± 0.20-fold, and 1.41 ± 0.18-fold, respectively. Specifically, NLRP3, active caspase-1, and GSDMD-N were significantly increased in the Model group compared with the Normal group ($P < 0.001$), whereas ASC showed a significant increase at $P < 0.01$. OA significantly reduced NLRP3 and ASC expression compared with the Model group ($P < 0.05$), while active caspase-1 and GSDMD-N were reduced at $P < 0.01$ (Figure 7B).

Dot blot analysis further revealed that global m6A levels were significantly increased in periodontal tissues from the Model group, reaching 2.38 ± 0.26-fold of the Normal level ($P < 0.001$), whereas OA treatment reduced this value to 1.42 ± 0.20-fold ($P < 0.01$ vs. Model; Figure 7C,D).

Consistent with these findings, immunohistochemical staining showed stronger METTL3 and NLRP3 immunoreactivity in periodontal ligament tissues from the Model group than in the Normal group. Quantitative analysis indicated that METTL3 and NLRP3 staining intensities increased to 3.12 ± 0.35-fold and 2.89 ± 0.31-fold of the Normal level, respectively ($P < 0.001$), and were reduced to 1.48 ± 0.21-fold and 1.39 ± 0.19-fold after OA treatment ($P < 0.01$ vs. Model; Figure 7E,F). Together, these findings further indicate that OA suppresses NLRP3 inflammasome activation and m6A hypermethylation in vivo.

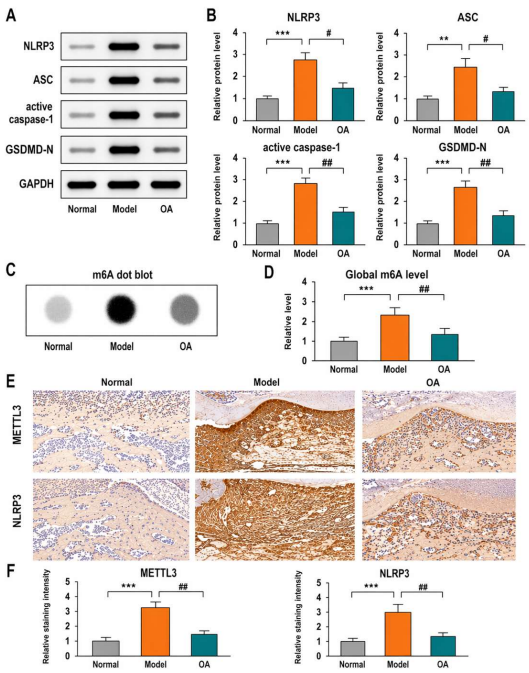

Figure 7. OA inhibits NLRP3 inflammasome activation and m6A hypermethylation in periodontal tissues. (A) Representative Western blot analysis of NLRP3, ASC, active caspase-1, GSDMD-N, and GAPDH in periodontal tissues from the Normal, Model, and OA groups. (B) Densitometric quantification of NLRP3, ASC, active caspase-1, and GSDMD-N normalized to GAPDH. (C) Representative dot blot analysis of global m6A levels in periodontal tissues. (D) Quantification of relative m6A dot blot signals. (E) Representative immunohistochemical staining of METTL3 and NLRP3 in periodontal ligament tissues from the Normal, Model, and OA groups. (F) Quantification of METTL3 and NLRP3 staining intensity. Data are presented as mean ± SD. **$P < 0.01$, ***$P < 0.001$ vs. Normal; #$P < 0.05$, ##$P < 0.01$ vs. Model.

3. Discussion

Periodontitis is a chronic inflammatory disease characterized by dysregulated host immune responses and progressive destruction of tooth-supporting tissues[27]. Despite advances in treatment, the development of effective host-modulating therapies remains an important clinical goal[28]. In this study, we demonstrate that oleic acid (OA) protects against Pg-LPS-induced pyroptosis in hPDLCs and

attenuates alveolar bone loss in a rat periodontitis model in association with altered m6A RNA methylation and suppression of the NLRP3 inflammasome pathway. These findings suggest that m6A dysregulation may be involved in periodontal inflammation and support the therapeutic potential of OA as a host-modulating strategy for periodontitis.

Pyroptosis, a lytic form of programmed cell death executed by gasdermin proteins, has emerged as a important contributor of inflammatory tissue destruction in periodontitis[7, 29]. Our results demonstrated that Pg-LPS induces pyroptosis in hPDLCs, as evidenced by increased NLRP3 and ASC expression, caspase-1 activation, GSDMD cleavage, and LDH release, along with elevated IL-1β and IL-18 secretion. These findings are consistent with previous studies showing that *P. gingivalis* virulence factors activate the NLRP3 inflammasome in periodontal cells[30, 31]. Ding et al. reported that *P. gingivalis*-induced NLRP3 inflammasome activation depends on caspase-4 in human macrophages[32], while Yamaguchi et al. demonstrated NLRP3 inflammasome regulation in *P. gingivalis*-accelerated periodontal disease[33]. Importantly, OA treatment significantly attenuated these pyroptosis-associated changes, indicating that OA exerts cytoprotective effects, at least in part, through suppression of inflammasome-mediated cell death.

The NLRP3 inflammasome is a important mediator of inflammatory responses in periodontitis[34]. Upon activation, NLRP3 oligomerizes with ASC to recruit pro-caspase-1, leading to caspase-1 autoproteolysis and subsequent cleavage of pro-IL-1β, pro-IL-18, and GSDMD[35]. Our Western blot analyses showed that Pg-LPS upregulated NLRP3, ASC, active caspase-1, and GSDMD-N in hPDLCs and rat periodontal tissues, and OA treatment significantly reduced all these components. These results are in line with recent reports that OA inhibits NLRP3 inflammasome activation in other cell types[36, 37] and further support a similar inhibitory effect of OA in hPDLCs and periodontal tissues.

A notable finding of our study was the involvement of m6A RNA methylation in Pg-LPS-induced pyroptosis and its modulation by OA. m6A was the most abundant internal mRNA modification and played diverse roles in RNA metabolism and gene expression[38]. Emerging evidence implicated m6A in inflammatory diseases by regulating the expression of cytokines and immune-related genes[14, 39]. Here, we found that Pg-LPS stimulation induces m6A hypermethylation in hPDLCs, accompanied by upregulation of METTL3 and METTL14 and downregulation of FTO and ALKBH5. In rat periodontal tissues, Pg-LPS-induced periodontitis was also associated with increased global m6A levels and enhanced METTL3 expression. These alterations were attenuated, with the most consistent effect observed for METTL3 suppression by OA treatment, suggesting that OA partially modulates m6A homeostasis.

The functional significance of m6A modification in inflammasome regulation is supported by recent studies. Yand et al. demonstrated that METTL3-mediated m6A methylation promotes NLRP3 inflammasome activation in macrophages by enhancing NLRP3 mRNA stability[15]. Using methylated RNA immunoprecipitation sequencing (MeRIP-seq), they identified m6A modification sites in the 3'UTR of NLRP3 mRNA and showed that METTL3 knockdown reduced NLRP3 expression and IL-1β secretion. Similarly, Zhang et al. reported that METTL3 inhibition suppresses NLRP3-mediated pyroptosis and alleviates myocardial ischemia-reperfusion injury[40]. Our observation that OA reduces METTL3 expression while only modestly affecting FTO and not reversing ALKBH5 expression suggests a potential link between m6A modulation and inflammasome suppression. The concurrent reduction of both METTL3 and NLRP3 protein expression in vivo following OA treatment, as demonstrated by immunohistochemistry, further supports this relationship. We speculate that OA may exert its protective effects by downregulating METTL3, thereby potentially reducing m6A-dependent regulation of NLRP3 and consequently attenuating inflammasome activation and pyroptosis.

The in vivo relevance of our findings was further supported in a rat ligature-induced periodontitis

model, which closely mimics human periodontitis pathology[41]. OA administration significantly attenuated alveolar bone loss, improved bone microarchitecture parameters (BV/TV,Tb.Th,Tb.Sp, BMD), and reduced inflammatory cytokine levels in serum. These protective effects were associated with reduced expression of NLRP3 inflammasome-related proteins and decreased global m6A levels in periodontal tissues. Notably, these protective effects are also consistent with previous reports showing that established host-modulatory agents, such as resolvins and lipoxins, can attenuate inflammatory bone loss in periodontitis models[42, 43].

The anti-inflammatory properties of oleic acid have been documented in various disease contexts. OA has been shown to reduce LPS-induced inflammatory responses in macrophages[44], protect against colitis in mice[20], and attenuate cartilage degradation in osteoarthritis models[19]. In the context of oral health, Huang et al. demonstrated that OA exhibits antibacterial effects against oral pathogens including *P. gingivalis*, *Aggregatibacter actinomycetemcomitans*, and *Fusobacterium nucleatum*, and reduces IL-6 and IL-8 production in human gingival fibroblasts stimulated with *P. gingivalis* LPS[45]. Our study extends these observations by suggesting potential mechanistic involvement of both pyroptosis regulation and epigenetic modification, and by showing protective effects in an in vivo periodontitis model. Given that OA is a naturally occurring dietary fatty acid with an generally favorable safety profile and is already widely consumed in Mediterranean diets, these findings suggest potential translational relevance for periodontitis management and may provide a rationale for OA-based host-modulating or nutritional approaches.

The crosstalk between m6A methylation and NLRP3-mediated pyroptosis suggested in this study adds to the growing understanding of epigenetic regulation in inflammatory diseases. Recent studies have implicated m6A modification as a important regulator of immune responses[13]. Our finding that OA modulates METTL3 expression suggests that targeting m6A writers may have therapeutic relevance in inflammatory diseases, particularly in the context of periodontal inflammation.

Several limitations of this study should be acknowledged. First, while we demonstrate associations between m6A modification and inflammasome activation, the precise molecular mechanism by which m6A regulates NLRP3 expression in periodontal cells requires further investigation. Future studies using m6A profiling approaches, such as methylated RNA immunoprecipitation sequencing (MeRIP-seq), and RNA immunoprecipitation (RIP-qPCR) could identify specific m6A-modified transcripts involved in inflammasome regulation and confirm whether NLRP3 mRNA is directly targeted by METTL3-mediated methylation. Second, although our data show that OA modulates multiple m6A regulators, the relative contributions of individual writers and erasers to the observed effects remain to be determined. Gain- and loss-of-function experiments targeting METTL3 and other candidate m6A regulators individually would help elucidate their specific roles. Third, although our data suggest a link between METTL3-associated m6A regulation and NLRP3 inflammasome activation, direct causal validation using targeted genetic or pharmacological intervention was not performed in the present study. Fourth, the optimal dosing regimen, bioavailability, route of administration, and long-term safety of OA for periodontitis treatment warrant further evaluation in larger animal studies and future clinical investigations.

5. Conclusion

In summary, this study demonstrates that oleic acid protects against periodontal destruction in vitro and in vivo. This study is the first to report an association between m6A methylation reprogramming and NLRP3-mediated pyroptosis in periodontitis, and identifies the m6A-NLRP3 axis as a potential target of oleic acid. These findings provide a rationale for exploring dietary interventions with oleic acid and lay the groundwork for future studies aimed at dissecting the direct molecular targets of OA in regulating epigenetic modifications.

References

[1] Y.L. Dong, H. Lin, T. Wen, Z.L. Guo, Multi-dimensional role of AGEs in periodontitis: from matrix remodeling to neuro-immune crosstalk, Front Immunol 16 (2025) 1643685.

[2] L.J. Suarez, P.K. Vargas-Sanchez, N. Angelov, E. Mylonakis, R.M. Arce, Host-pathogen interactions in periodontitis: an integrative interkingdom perspective, Front Immunol 17 (2026) 1797726.

[3] J. Feng, D. Fu, S. Phan, X. Hu, Q. Xing, P. Gingivalis LPS Drives Osteoclastogenesis and Impairs Osteoblast Differentiation by Suppressing Sema3A/Nrp1 Via TLR-4, Int Dent J 75(6) (2025) 103941.

[4] E.N. Kim, N.M. Trang, M. Na, G.S. Jeong, Pharmacological investigation of bergapten isolated from Glehnia littoralis against periodontitis, Sci Rep 16(1) (2026).

[5] Y. Huang, Y. Tang, R. Zhang, X. Wu, L. Yan, X. Chen, Q. Wu, Y. Chen, Y. Lv, Y. Su, Role of periodontal ligament fibroblasts in periodontitis: pathological mechanisms and therapeutic potential, J Transl Med 22(1) (2024) 1136.

[6] S. Corbella, E. Calciolari, A. Alberti, N. Donos, L. Francetti, Systematic review and meta-analysis on the adjunctive use of host immune modulators in non-surgical periodontal treatment in healthy and systemically compromised patients, Sci Rep 11(1) (2021) 12125.

[7] Y. Qie, J. Li, Y. Xu, S. Liu, N. Liu, Q. Liu, Targeting pyroptosis in periodontitis: mechanisms and therapeutic strategies, Front Immunol 17 (2026) 1761693.

[8] P. Broz, Pyroptosis: molecular mechanisms and roles in disease, Cell Res 35(5) (2025) 334-344.

[9] H.J. Shin, I.S. Kim, J.K. Kim, E.K. Jo, Molecular mechanisms of NLRP3 inflammasome activation, Exp Mol Med 58(3) (2026) 650-663.

[10] H. Zhan, G. Shi, Q. Xie, Y. Chen, Y. Zhang, ELAVL1 modulates periodontal ligament fibroblast pyroptosis in periodontitis through the JAK2/STAT3/NLRP3 axis, Int Immunol (2026).

[11] R. Kansal, V. Sharma, P. Potraje, M. Datta, m6A RNA modification and its emerging roles in diseases: recent advances and therapeutic implications, J Transl Med 24(1) (2026).

[12] Y. Sun, J. Wu, G. Chen, H. Ma, W. Li, H. Tan, K. Yang, Rewriting the RNA code: an m(6)a-centric framework to classify tumors and guide combination therapies, Front Immunol 17 (2026) 1749911.

[13] D. Srivastava, V. Nayak, S. Pahari, G. Sandeep, A. Misra, Epitranscriptomic regulation of immunity: The role of m6A in shaping immune response dynamics, Cytokine 194 (2025) 157011.

[14] Z. Li, Y. Lao, R. Yan, F. Li, X. Guan, Z. Dong, N6-methyladenosine in inflammatory diseases: Important actors and regulatory targets, Gene 936 (2025) 149125.

[15] Q. Yang, J. Xiao, Y. Liu, Z. Yang, C. Wang, J. Sun, H. Wang, H. Liu, X. Wang, L. Ma, X. Huang, Z. Cao, METTL3-mediated m6A modifications of NLRP3 accelerate alveolar bone resorption through enhancing macrophage pyroptosis, Cell Signal 127 (2025) 111572.

[16] S.Y. Lee, D.D. Le, C.S. Bae, J.W. Park, M. Lee, S.S. Cho, D.H. Park, Oleic acid attenuates asthma pathogenesis via Th1/Th2 immune cell modulation, TLR3/4-NF-κB-related inflammation suppression, and intrinsic apoptotic pathway induction, Front Immunol 15 (2024) 1429591.

[17] C. Santa-María, S. López-Enríquez, S. Montserrat-de la Paz, I. Geniz, M.E. Reyes-Quiroz, M. Moreno, F. Palomares, F. Sobrino, G. Alba, Update on Anti-Inflammatory Molecular Mechanisms Induced by Oleic Acid, Nutrients 15(1) (2023).

[18] X. Li, C. Zhao, C. Mao, G. Sun, F. Yang, L. Wang, X. Wang, Oleic and linoleic acids promote chondrocyte apoptosis by inhibiting autophagy via downregulation of SIRT1/FOXO1 signaling, Biochim Biophys Acta Mol Basis Dis 1870(4) (2024) 167090.

[19] Y.M. Bastiaansen-Jenniskens, M. Siawash, C.H. van de Lest, J.A. Verhaar, M. Kloppenburg, A.M. Zuurmond, V. Stojanovic-Susulic, G.J. Van Osch, S. Clockaerts, Monounsaturated and Saturated, but Not n-6 Polyunsaturated Fatty Acids Decrease Cartilage Destruction under Inflammatory Conditions: A Preliminary Study, Cartilage 4(4) (2013) 321-8.

[20] M. Xia, Y. Liu, X. Zhao, Q. Du, Z. Chen, J. Wang, K. Ghoreschi, A. Laurence, X. Xiong, J. Zhang, M. Zeng, X.P. Yang, Oleic Acid Promotes Treg Cell Differentiation via Autophagy Induction and Ameliorates DSS-Induced Colitis, Eur J Immunol 56(3) (2026) e70173.

[21] A. Döding, L. Wurschi, C. Zubiria-Barrera, T.E. Klassert, L. Bereuter, Z. Rao, A.K. Bär, A. Domuncu, A. Koeberle, H. Noels, H. Slevogt, B. Sigusch, U. Schulze-Späte, Mediterranean diet component oleic acid decreases systemic impact of periodontal Porphyromonas gingivalis-infection in age: addressing role of stress resistance and microbiome, NPJ Aging 11(1) (2025) 54.

[22] J. Lu, Y. Hu, Z. Tang, C. Zhang, L. Jin, M. Gu, Y. Yang, Porphyromonas gingivalis lipopolysaccharide enhances the proliferation of human periodontal ligament cells via upregulation of cyclin D1, cyclin A and cyclin B1, Exp Ther Med 23(1) (2022) 2.

[23] Y.G. Liu, J.K. Chen, Z.T. Zhang, X.J. Ma, Y.C. Chen, X.M. Du, H. Liu, Y. Zong, G.C. Lu, NLRP3 inflammasome activation mediates radiation-induced pyroptosis in bone marrow-derived macrophages, Cell Death Dis 8(2) (2017) e2579.

[24] A. Nagarajan, R. Janostiak, N. Wajapeyee, Dot Blot Analysis for Measuring Global N(6)-Methyladenosine Modification of RNA, Methods Mol Biol 1870 (2019) 263-271.

[25] A. Kuhr, A. Popa-Wagner, H. Schmoll, C. Schwahn, T. Kocher, Observations on experimental marginal periodontitis in rats, J Periodontal Res 39(2) (2004) 101-6.

[26] I.M. Medeiros-de-Moraes, C.F. Gonçalves-de-Albuquerque, A.R.M. Kurz, F.M.J. Oliveira, V.H.P. de Abreu, R.C. Torres, V.F. Carvalho, V. Estato, P.T. Bozza, M. Sperandio, H.C. de Castro-Faria-Neto, A.R. Silva, Omega-9 Oleic Acid, the Main Compound of Olive Oil, Mitigates Inflammation during Experimental Sepsis, Oxid Med Cell Longev 2018 (2018) 6053492.

[27] R.S. de Molon, R. Vernal, G.E. Oliveira, J.P. Steffens, E. Ervolino, L.H. Theodoro, J. van den Beucken, S. Tetradis, Inflammatory bone loss and signaling pathways in periodontitis: mechanistic insights and emerging therapeutic strategies, Bone Res 14(1) (2026) 1.

[28] A. Phanrungsuwan, J. Huang, N. Dharmaraj, A. Cobos Perez, O. Veiseh, S. Young, C.T. Lee, Host modulation therapy in periodontitis: from established therapies to emerging technologies, Front Immunol 17 (2026) 1762187.

[29] P. Chen, D. Liu, Y.K. Zhou, J.H. Jiang, R.L. Yang, Pyroptosis of periodontal ligament stem cells aggravates periodontitis via Piezo1 channel, iScience 28(5) (2025) 112395.

[30] K. Yang, S. Xu, H. Zhao, L. Liu, X. Lv, F. Hu, L. Wang, Q. Ji, Hypoxia and Porphyromonas gingivalis-lipopolysaccharide synergistically induce NLRP3 inflammasome activation in human gingival fibroblasts, Int Immunopharmacol 94 (2021) 107456.

[31] X. Lv, C. Fan, Z. Jiang, W. Wang, X. Qiu, Q. Ji, Isoliquiritigenin alleviates P. gingivalis-LPS/ATP-induced pyroptosis by inhibiting NF-κB/ NLRP3/GSDMD signals in human gingival fibroblasts, Int Immunopharmacol 101(Pt B) (2021) 108338.

[32] P.H. Ding, M.X. Yang, N.N. Wang, L.J. Jin, Y. Dong, X. Cai, L.L. Chen, Porphyromonas gingivalis-Induced NLRP3 Inflammasome Activation and Its Downstream Interleukin-1β Release Depend on Caspase-4, Front Microbiol 11 (2020) 1881.

[33] Y. Yamaguchi, T. Kurita-Ochiai, R. Kobayashi, T. Suzuki, T. Ando, Regulation of the NLRP3 inflammasome in Porphyromonas gingivalis-accelerated periodontal disease, Inflamm Res 66(1) (2017) 59-65.

[34] K. Jayaprakash Demirel, R. Wu, A. Neves Guimaraes, I. Demirel, The role of NLRP3 in regulating gingival epithelial cell responses evoked by Aggregatibacter actinomycetemcomitans, Cytokine 169 (2023) 156316.

[35] J. Yao, K. Sterling, Z. Wang, Y. Zhang, W. Song, The role of inflammasomes in human diseases and their potential as therapeutic targets, Signal Transduct Target Ther 9(1) (2024) 10.

[36] L. L'Homme, N. Esser, L. Riva, A. Scheen, N. Paquot, J. Piette, S. Legrand-Poels, Unsaturated fatty

acids prevent activation of NLRP3 inflammasome in human monocytes/macrophages, J Lipid Res 54(11) (2013) 2998-3008.
[37] X. Zeng, M. Zhu, X. Liu, X. Chen, Y. Yuan, L. Li, J. Liu, Y. Lu, J. Cheng, Y. Chen, Oleic acid ameliorates palmitic acid induced hepatocellular lipotoxicity by inhibition of ER stress and pyroptosis, Nutr Metab (Lond) 17 (2020) 11.
[38] S. Wang, W. Lv, T. Li, S. Zhang, H. Wang, X. Li, L. Wang, D. Ma, Y. Zang, J. Shen, Y. Xu, W. Wei, Dynamic regulation and functions of mRNA m6A modification, Cancer Cell Int 22(1) (2022) 48.
[39] L. Zhang, W. Chen, Y. Liu, S. Zhang, B. Yin, K. Liu, X. Gu, X. Hu, Research advances in m(6)A methylation and sepsis, Front Cell Dev Biol 13 (2025) 1682283.
[40] X. Wang, Y. Li, J. Li, S. Li, F. Wang, Mechanism of METTL3-Mediated m(6)A Modification in Cardiomyocyte Pyroptosis and Myocardial Ischemia-Reperfusion Injury, Cardiovasc Drugs Ther 37(3) (2023) 435-448.
[41] F. Khuda, B. Baharin, N.N.M. Anuar, B.S.F. Satimin, N.S. Nasruddin, Effective Modalities of Periodontitis Induction in Rat Model, J Vet Dent 41(1) (2024) 49-57.
[42] E. Börgeson, J. Lönn, I. Bergström, V.P. Brodin, S. Ramström, F. Nayeri, E. Särndahl, T. Bengtsson, Lipoxin A_4 inhibits porphyromonas gingivalis-induced aggregation and reactive oxygen species production by modulating neutrophil-platelet interaction and CD11b expression, Infect Immun 79(4) (2011) 1489-97.
[43] C.T. Lee, R. Teles, A. Kantarci, T. Chen, J. McCafferty, J.R. Starr, L.C. Brito, B.J. Paster, T.E. Van Dyke, Resolvin E1 Reverses Experimental Periodontitis and Dysbiosis, J Immunol 197(7) (2016) 2796-806.
[44] A.K. Müller, F. Albrecht, C. Rohrer, A. Koeberle, O. Werz, W. Schlörmann, M. Glei, S. Lorkowski, M. Wallert, Olive Oil Extracts and Oleic Acid Attenuate the LPS-Induced Inflammatory Response in Murine RAW264.7 Macrophages but Induce the Release of Prostaglandin E2, Nutrients 13(12) (2021).
[45] C.B. Huang, B. George, J.L. Ebersole, Antimicrobial activity of n-6, n-7 and n-9 fatty acids and their esters for oral microorganisms, Arch Oral Biol 55(8) (2010) 555-60.

Author Contributions

Conceptualization, Shuwen Pan and Kon Ken Wong; methodology, Shuwen Pan; validation, Shuwen Pan, Fook Choe Cheah, and Kon Ken Wong; formal analysis, Shuwen Pan; investigation, Shuwen Pan; resources, Kon Ken Wong; data curation, Shuwen Pan; writing—original draft preparation, Shuwen Pan; writing—review and editing, Fook Choe Cheah and Kon Ken Wong; visualization, Shuwen Pan; supervision, Kon Ken Wong; project administration, Kon Ken Wong; funding acquisition, Kon Ken Wong. All authors have read and agreed to the published version of the manuscript.

Funding

No funding.

Institutional Review Board Statement

The study was conducted in accordance with the Declaration of Helsinki and approved by the Institutional Review Board of [University Name] (protocol code [XXX]; approved on [Date]). The animal study protocol was approved by the Institutional Animal Care and Use Committee of [University Name] (protocol code [XXX]; approved on [Date]).

Informed Consent Statement

Informed consent was obtained from all subjects or their legal guardians involved in the study.

Data Availability Statement

The data presented in this study are available in the article and supplementary materials. Original Western blot images and raw data are available from the corresponding author upon reasonable request.

Conflicts of Interest

The authors declare no conflicts of interest. The funders had no role in the design of the study; in the collection, analyses, or interpretation of data; in the writing of the manuscript; or in the decision to publish the results.

References

Figure Legends

Figure 1. Oleic acid attenuates Pg-LPS-induced cytotoxicity and pyroptosis in hPDLCs. (A) Cell viability measured by CCK-8 assay. (B) LDH release in culture supernatants. (C) Representative flow cytometry plots of FAM-FLICA caspase-1/PI staining in the Control, Pg-LPS, and Pg-LPS+OA groups. (D) Quantification of pyroptosis rate. Data are presented as mean ± SD (n = 3). ***p < 0.001 vs. Control; ##p < 0.01 vs. Pg-LPS.

Figure 2. OA suppresses Pg-LPS-induced inflammatory cytokine secretion in hPDLCs. (A) IL-1β levels in culture supernatants measured by ELISA. (B) IL-18 levels in culture supernatants measured by ELISA. Data are presented as mean ± SD (n = 3). **P < 0.01, ***P < 0.001 vs. Control; ##P < 0.01, ###P < 0.001 vs. Pg-LPS.

Figure 3. OA inhibits NLRP3 inflammasome activation in Pg-LPS-stimulated hPDLCs. (A) Representative Western blot analysis of NLRP3, ASC, active caspase-1 (p10), GSDMD-N, and GAPDH in hPDLCs. (B) Densitometric quantification of protein bands normalized to GAPDH (n = 3). Data are presented as mean ± SD. **P < 0.01, ***P < 0.001 vs. Control; #P < 0.05, ##P < 0.01 vs. Pg-LPS.

Figure 4. OA modulates global m6A RNA methylation and m6A-related regulators in Pg-LPS-stimulated hPDLCs. (A) Representative dot blot analysis of global m6A levels in hPDLCs. (B) Quantification of relative m6A dot blot signals. (C) qRT-PCR analysis of m6A-related regulators, including METTL3, METTL14, WTAP, RBM15, FTO, and ALKBH5. (D) Representative Western blot analysis of METTL3 protein expression. (E) Densitometric quantification of METTL3 normalized to GAPDH. Data are presented as mean ± SD (n = 3). *P < 0.05, **P < 0.01, ***P < 0.001 vs. Control; ##P < 0.01 vs. Pg-LPS.

Figure 5. OA attenuates alveolar bone loss and improves periodontal tissue integrity in a rat periodontitis model. (A) Quantification of the distance from the cementoenamel junction to the alveolar bone crest (CEJ-ABC). (B) Bone volume fraction (BV/TV). (C) Trabecular thickness (Tb.Th). (D) Trabecular separation (Tb.Sp). (E) Trabecular number (Tb.N). (F) Bone mineral density (BMD). (G) Representative hematoxylin and eosin (H&E) staining images of periodontal tissues from the Normal, Model, and OA groups. Data in (A–F) are presented as mean ± SD (n = 6). P < 0.01, *P < 0.001 vs. Normal; #P < 0.05, ##P < 0.01 vs. Model.

Figure 6. OA suppresses systemic inflammation in the rat periodontitis model. Serum levels of (A) TNF-α, (B) IL-1β, (C) IL-6, and (D) IL-18 were measured by ELISA. Data are presented as mean ± SD (n = 6). **P < 0.01, ***P < 0.001 vs. Normal; #P < 0.05, ##P < 0.01 vs. Model.

Figure 7. OA inhibits NLRP3 inflammasome activation and m6A hypermethylation in periodontal tissues. (A) Representative Western blot analysis of NLRP3, ASC, active caspase-1, GSDMD-N, and GAPDH in periodontal tissues from the Normal, Model, and OA groups. (B) Densitometric quantification of NLRP3, ASC, active caspase-1, and GSDMD-N normalized to GAPDH. (C) Representative dot blot analysis of global m6A levels in periodontal tissues. (D) Quantification of relative m6A dot blot signals. (E) Representative immunohistochemical staining of METTL3 and NLRP3 in periodontal ligament tissues from the Normal, Model, and OA groups. (F) Quantification of METTL3 and NLRP3 staining intensity. Data are presented as mean ± SD. **P < 0.01, ***P < 0.001 vs. Normal; #P < 0.05, ##P < 0.01 vs. Model.